

Approaching actinide(+III) hydration from first principles

J. Wiebke,^a A. Moritz,^a X. Cao,^a and M. Dolg ^{a*}

^a *Institute for Theoretical Chemistry, Universität zu Köln,*

Greinstr. 4, D-50939 Cologne, Germany

(Dated: November 14, 2006)

Abstract

A systematic computational approach to An^{III} hydration on a density-functional level of theory, using quasi-relativistic 5f-in-core pseudopotentials and valence-only basis sets for the An^{III} subsystems, is presented. Molecular structures, binding energies, hydration energies, and Gibbs free energies of hydration have been calculated for $[\text{An}^{\text{III}}(\text{OH}_2)_h]^{3+}$ ($h = 7, 8, 9$) and $[\text{An}^{\text{III}}(\text{OH}_2)_{h-1} \cdot \text{OH}_2]^{3+}$ ($h = 8, 9$), using large (7s6p5d2f1g)/[6s5p4d2f1g] An^{III} and cc-pVQZ O and H basis sets within the COSMO implicit solvation model. An^{III} preferred primary hydration numbers are found to be 8 for all An^{III} at the gradient-corrected density-functional level of theory. Second-order Møller–Plesset perturbation theory predicts preferred primary hydration numbers of 9 and 8 for $\text{Ac}^{\text{III}}\text{--Md}^{\text{III}}$ and $\text{No}^{\text{III}}\text{--Lr}^{\text{III}}$, respectively.

*E-mail:m.dolg@uni-koeln.de

I. INTRODUCTION.

The relevance of actinide chemistry is mainly due to nuclear power generation [1, 2] and the related problems of spent nuclear fuel reprocessing [3] and nuclear waste disposal [4]. Particularly, outside lanthanide–lanthanide and actinide–actinide separation chemistry [5, 6], it is environmental actinide chemistry [7] that is of increasing importance. Whereas the majority of actinide separation processes relies heavily on liquid–liquid extraction techniques from or into the aqueous phase, the main risk of long-term nuclear waste disposal is soil contamination by nuclear material migration *via* natural ground water systems. It is thus clear that, although not sufficient, an in-depth understanding of actinide aqueous chemistry and hydration is necessary for the development of advanced actinide separation processes, safe and economic disposal strategies, and the prediction of actinide environmental behavior. It is the aqueous chemistry of actinide(+III) systems that is of special importance, since +III is the thermodynamically most stable oxidation state of all transplutonium actinides relevant to nuclear industry, and is known for most actinides in general [8].

An^{III} hydration is still poorly understood. Experimentally, only the subset U^{III}–Cf^{III} has been investigated mainly by means of extended X-ray absorption spectroscopy (EXAFS) [9–15] and time-resolved laser fluorescence (TRLF) spectroscopy [16, 17]. An^{III} coordination numbers are reported to range from 8 to 10, commonly with accuracies of *ca.* ± 1 , and vary irregularly over the subset investigated. Moreover, EXAFS coordination numbers might be considered as somewhat model-dependent due to the nature of the EXAFS experiment [18]. Mean An^{III}–O distances reported are in satisfactory agreement within *ca.* ± 2 pm and give a consistent general trend; however, no molecular structure data can be obtained from EXAFS and TRLFS. Therefore, and in view of actinide radiotoxicity and vanishing availability with increasing nuclear charge number, it is desirable that computational chemistry supports the experimental investigations. However, computational studies are quite demanding due to the need to address both the substantial relativistic and correlation effects as well as the potentially large number of unpaired electrons in the open 5f shells. Only Ac^{III} [19], Np^{III} [10], Pu^{III} [20], and Cm^{III} systems [21] have been studied so far, mainly on density-functional levels of theory; other studies [22–24] are of interest mainly from an electronic-structure theory point of view. Whereas calculated coordination numbers agree with the experimental 8–10 interval [10, 20, 21], An^{III}–O distances are systematically overestimated due to the

neglect of bulk solvation effects [19, 21], and molecular structures are commonly calculated within heavy symmetry constraints in order to limit the otherwise high computational costs.

We report here the first systematic quantum chemical study of An^{III} hydration for all elements of the series from first principles. We have modeled the hydrated An^{III} species as polyaquaaactinide(+III) systems $[\text{An}^{\text{III}}(\text{OH}_2)_h]^{3+}$, considering $h = 7, 8, \text{ and } 9$, to come to molecular structure parameters and binding energies. Hydration energies, Gibbs free energies of hydration, and preferred An^{III} primary hydration numbers h^* have been calculated by addressing bulk solvation effects *via* the polarizable continuum model (PCM) COSMO [25, 26]. We used quasi-relativistic An^{III} 5f-in-core pseudopotentials (PPs) recently developed in our group [24] together with routine quantum chemistry density-functional theory (DFT) methods and programs. In a somewhat simplified picture, within the 5f-in-core approximation we collect all An^{III} electrons with principal quantum numbers $n < 6$, including An^{III} open 5f shells, in the PP core giving rise to An^{III} $6s^2 6p^6 6d^0 7s^0$ effective 8-electron systems [24]. As it has been shown [19–24] that An^{III} 5f shells are of mainly atomic nature in $\text{An}^{\text{III}}\text{-OH}_2$ systems, and, more general, that single-reference and DFT methods appear to be applicable to open-shell actinide systems if one seeks ground state molecular structures and properties [27], we initially believed and report here that the 5f-in-core approximation on a DFT level of theory is justified for $[\text{An}^{\text{III}}(\text{OH}_2)_h]^{3+}$ systems.

II. COMPUTATIONAL DETAILS.

Our computational strategy to approach An^{III} hydration is as follows (cf. fig. 1). As a starting point, we calculated gas phase molecular structures and gas phase binding energies D_0 of $[\text{An}^{\text{III}}(\text{OH}_2)_h]^{3+}$, considering $h = 7, 8, \text{ and } 9$, and of $[\text{An}^{\text{III}}(\text{OH}_2)_{h-1} \cdot \text{OH}_2]^{3+}$, considering $h = 8 \text{ and } 9$ only. Hydration energies ΔE_{H} and Gibbs free energies of hydration were approximated by single-point energy calculations for fixed gas phase molecular structures within the COSMO Self-Consistent Reaction Field (SCRF). From these energies, preferred An^{III} primary hydration numbers h^* were calculated from the $[\text{An}^{\text{III}}(\text{OH}_2)_{h-1} \cdot \text{OH}_2]^{3+} \longrightarrow [\text{An}^{\text{III}}(\text{OH}_2)_h]^{3+}$ reaction.

All calculations were carried out with the TURBOMOLE v. 5.6 and v. 5.7 program packages [28]. For all An^{III} , quasi-relativistic energy-consistent 5f-in-core PPs and corresponding An^{III} valence-only (5s5p4d)/[4s4p3d] GTO basis sets [24] with extra 2, 1, and 1 diffuse s, p,

and d functions, and 2 f polarization functions, *i.e.*, (7s6p5d2f)/[6s5p4d2f] basis sets were used; for O and H, small aug-cc-pVDZ basis sets [29] were used. For BP86-DFT single-point energy calculations, 1 g polarization function was added to the An^{III} basis sets, and for O and H large cc-pVQZ basis sets were used. It has been shown [30] that this calculation scheme provides molecular structures very close to the An^{III} (7s6p5d2f1g)/[6s5p4d2f1g] and O and H cc-pVQZ case, the diffuse O and H basis functions compensating for the lack of larger O and H angular momentum polarization functions, whereas total energies come close to the fully uncontracted basis set total energies. BSSE corrections to gas phase binding energies were found to remain below *ca.* 0.05 eV. DFT with BP86 exchange–correlation [31–35] was chosen as a general level of theory because of favorable computational performance compared to hybrid-type functionals as well as the good unscaled frequencies to be expected [36]. For numerical BP86-DFT XC term quadrature the TURBOMOLE v. 5.6 and v. 5.7 lanthanum dynamic m5 grid was used for all An^{III}. SCF thresholds were set to 10⁻⁷ a.u. Molecular structures were optimized without any symmetry constraints until the internal gradient norms dropped below 10⁻³ a.u., and were confirmed as true potential energy surface minima by numerical frequency analysis with the TURBOMOLE NUMFORCE module. For all An^{III}, only most stable nuclide’s masses [37] were considered. Entropy calculations were carried out for $T = 298.15$ K, $p = 0.1$ MPa. For the sake of a qualitative measure of DFT binding energies single-point energy calculations were carried out also at the MP2 level of theory, using the small An^{III} (7s6p5d2f)/[6s5p4d2f] and O and H aug-cc-pVDZ basis sets only for computational efficiency. O 1s electrons were not correlated.

Single-point energy calculations with the COSMO PCM [25, 26] were carried out using infinite permittivity and the COSMO default parameter set. The An^{III} PCM cavity radii r were obtained as follows: For all atomic An^{III} BP86-DFT single-point energy calculations were carried out without and with the COSMO SCRF for varying r , using large An^{III} (8s7p6d2f1g)/[6s5p5d2f1g] basis sets. An^{III} r were then chosen as to match semiempirical An^{III} Gibbs free energies of hydration [38] with the COSMO SCRF energies obtained (cf. tab. I). No physical significance is attributed to the set of An^{III} r obtained, although we assume consistency over the An^{III} series because of the qualitatively correct thermodynamic trends incorporated. For O and H, the recommended [25] r of 172 and 130 pm were used, respectively.

III. RESULTS AND DISCUSSION.

A. An^{III}-aqua ion molecular and electronic structure.

Considering primary hydration numbers h of 7, 8, and 9 in $[\text{An}^{\text{III}}(\text{OH}_2)_h]^{3+}$, among the set of possible coordination isomers only the most stable coordination isomers were considered (cf. fig. 2). For $h = 7$, no pentagonal bipyramid minimum, but 1-capped trigonal prism **1** and antiprism minimum structures were found, which are degenerate within *ca.* 10^{-4} eV for the Ac^{III} and Lr^{III} systems. **1** was chosen as isomer of interest because of its higher symmetry. For $h = 8$, no square prism minimum structures were found; square antiprism structures **2** were found to be lower in total energy by 0.12 and 0.22 eV than the dodecahedron minimum structures for the Ac^{III} and Lr^{III} systems, respectively. Because of experimental [39] and theoretical evidence [21, 40–42], for $h = 9$ only 3-capped trigonal prism coordination isomers **3** were considered. For $h = 8$, the most stable coordination isomers do not agree with reported $[\text{An}^{\text{III}}(\text{OH}_2)_8]^{3+}$ molecular structures from symmetry-constrained calculations [10, 20, 21], but with corresponding $[\text{Ln}^{\text{III}}(\text{OH}_2)_8]^{3+}$ molecular structures within a similar 4f-in-core approximation [42], and Sm^{III} and Yb^{III} system molecular dynamics simulations [40]. The same is true for $h = 9$ which, however, matches the D_3 symmetric structure of Yang and Bursten [21]. For $h = 10$ and Pu^{III} no minimum structures could be found neither with nor without symmetry constraints.

Generally, OH₂ coordination in **1**, **2**, and **3** was found to be such that the An^{III}-O and OH₂ dipole vectors are parallel. Gas phase structure parameters vary monotonically with both h and Z (cf. tab. II, fig. 3). Mean An^{III}-O distances d_{AnO} increase with h and decrease with increasing Z for $h = 7, 8, \text{ and } 9$, by 24.1, 23.4, and 22.1 pm, respectively. The general trend is in line with fully relativistic studies of the actinide contraction [43], as well as 5f-in-core and 5f-in-valence PP studies [24]. It also agrees with fully relativistic all-electron studies [22, 23] of the related $[\text{An}^{\text{III}}(\text{OH}_2)]^{3+}$ systems. The effect of OH₂ coordination by An^{III} is such that mean O-H distances d_{OH} and mean HOH angles φ_{HOH} increase with respect to the free system OH₂. Whereas there is a tendency for d_{OH} to gradually decrease towards the free OH₂ d_{OH} with increasing h , there is a small increase of φ_{HOH} with both increasing Z and h (cf. electronic supplementary information). An^{III} Mulliken net charges increase with h and, for the second half of the An^{III} series, with Z (cf. fig. 4). Particularly,

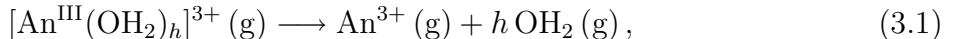
An^{III} 5f populations decrease from 0.14 to 0.05 with increasing Z which is to some extent an *a posteriori* justification of the 5f-in-core approximation. Note that the f terms of the pseudopotentials have been adjusted in such a way that slightly larger than integral 5f populations are allowed. O and H mean Mulliken net charges decrease and increase, respectively, with both increasing Z and h . The [An^{III}(OH₂) _{h}]³⁺ structure parameters and Mulliken net charges calculated are in line with the previously established electrostatic picture of the An^{III}-OH₂ interaction [22–24]. OH₂ coordination by the An^{III} Lewis acids increases φ_{HOH} for electrostatic reasons, whereas small φ_{HOH} support OH₂ 3a₁ → 6d donation. As 3a₁ → 6d contributions are generally small [22–24] and become less important with both increasing h and Z due to increasing OH₂-OH₂ repulsion and An^{III} 6d shell compactness, one finds increasing d_{OH} with increasing h , and increasing φ_{HOH} and An^{III} Mulliken net charges with increasing h and Z .

Compared with experimental EXAFS [9–15] and TRIFS [16, 17] data, calculated [An^{III}(OH₂) _{h}]³⁺ mean An^{III}-O distances d_{AnO} reproduce the global trend correctly, but are, however, too large systematically (cf. fig. 3). This is attributed to the neglect of bulk solvation effects [19, 21]. Therefore, as a model approach to higher hydration spheres, the study of the polyaquaaactinide(+III) [An^{III}(OH₂) _{h}]³⁺ was extended to the corresponding [An^{III}(OH₂) _{$h-1$} · OH₂]³⁺ systems, which coordinate $h - 1$ OH₂ ligands in the 1st and one single OH₂ ligand in the 2nd hydration sphere. [An^{III}(OH₂) _{$h-1$} · OH₂]³⁺ were modeled with the [An^{III}(OH₂) _{$h-1$}]³⁺ fragment coordinating OH₂ in an η^2 fashion. Considering $h = 8$ and 9 only, the most stable coordination isomers were found to be **4** and **5**, respectively (cf. fig. 2). Mean d_{AnO} for 1st sphere OH₂ ligands that coordinate the one 2nd sphere OH₂ ligand decrease with increasing Z for $h = 8$ and 9 from 257.6 to 234.5 pm and from 258.9 to 237.9 pm, *i.e.* by 23.1 and 21.0 pm, respectively (cf. tab. II). For these OH₂ ligands there is a small tendency for d_{OH} to increase with increasing Z for $h = 8$ and 9 from 100.8 to 101.1 and from 100.5 to 100.8 pm; φ_{HOH} increase for $h = 8$ and 9 from 105.7 to 106.8° and from 105.7 to 106.7°, respectively (cf. electronic supplementary information). O and H mean Mulliken net charges decrease and increase, respectively, both with increasing Z and h . The general trend is in line with the one discussed for the [An^{III}(OH₂) _{h}]³⁺ systems, but d_{AnO} for those 1st sphere OH₂ ligands which coordinate the single 2nd sphere OH₂ ligand are much closer to experimental data. Therefore, we believe that also d_{OH} , φ_{HOH} , and O and H Mulliken net charges correspond better to 1st hydration sphere properties of the hydrated An^{III} species,

since the single 2nd sphere OH₂ ligand serves as a local model for bulk solvation effects not addressed in the corresponding [An^{III}(OH₂)_h]³⁺ systems.

B. An^{III} binding energies, hydration energies, and Gibbs free energies of hydration.

According to



[An^{III}(OH₂)_h]³⁺ ZPE corrected gas phase binding energies D_0 values are given in tab. III. D_0 increase with both h and Z , because more OH₂ ligands are subjected to An^{III} coordination, and because of increasingly stronger An^{III}–OH₂ interaction, respectively. D_0/h , however, decreases with increasing h . Since D_0/h decreases, but An^{III} net charges increase with increasing h for given Z , the decrease of D_0/h is attributed to OH₂–OH₂ repulsion becoming more relevant with increasing h . In order to derive hydration energies ΔE_{H} , one has to consider [44]



i.e., with D_0 one neglects OH₂ and [An^{III}(OH₂)_h]³⁺ bulk phase interactions (cf. fig. 1). As a first-order approximation, bulk phase interactions were addressed by calculating OH₂ and [An^{III}(OH₂)_h]³⁺ total energies within the COSMO SCRf for fixed gas phase molecular structures. Then,

$$\Delta E_{\text{H}} \approx -D_0 + \Delta E^{\text{SCRf}} \quad (3.3)$$

where ΔE^{SCRf} is the difference of the COSMO SCRf contributions to h free OH₂ ligands and [An^{III}(OH₂)_h]³⁺ total energies, as given in tab. III. The ΔE^{SCRf} values are found to increase, *i.e.*, to become less negative with increasing h , which is attributed to the increasing molecular PCM cavity, but they follow the same general trend with increasing Z as the $-D_0$ values do. The An^{III} hydration energies ΔE_{H} , however, are found to be very similar for different h , and almost identical for $h = 8$ and 9 and late An^{III} species (cf. fig. 5). This is because, with increasing h , more OH₂ ligands must be brought out of the COSMO SCRf for An^{III}–OH₂ coordination to occur in the gas phase (cf. fig. 1); with increasing h , on the other hand, [An^{III}(OH₂)_h]³⁺ SCRf energies become more positive. Therefore, large parts of the [An^{III}(OH₂)_h]³⁺ D_0 differences due to different h are compensated both by the formal

process $h \text{OH}_2 (\text{aq}) \longrightarrow h \text{OH}_2 (\text{g})$ and the decrease of SCRF stabilization with increasing h . Particularly, it is this subtle interplay of SCRF energy differences that causes ΔE_{H} for $h = 8$ to outrun ΔE_{H} for $h = 9$ for late An^{III} species. Although tempting, from this data one cannot come to preferred An^{III} hydration numbers h^* , since from D_0 and ΔE_{H} one cannot interpolate to *successive* OH_2 binding energies. Instead, one has to consider the competing addition of OH_2 ligands in the 2nd hydration sphere as well.

For $[\text{An}^{\text{III}}(\text{OH}_2)_{h-1} \cdot \text{OH}_2]^{3+}$, the gas phase binding energies D_0 follow the same general trend as discussed for the $[\text{An}^{\text{III}}(\text{OH}_2)_h]^{3+}$ systems. The D_0 values increase with both h and Z , but D_0/h decreases with increasing h . Outside the general trend, however, $[\text{An}^{\text{III}}(\text{OH}_2)_{h-1} \cdot \text{OH}_2]^{3+}$ D_0 are found to be more negative than the corresponding $[\text{An}^{\text{III}}(\text{OH}_2)_h]^{3+}$ D_0 , indicating the h^{th} OH_2 ligand being more tightly bound to the $[\text{An}^{\text{III}}(\text{OH}_2)_{h-1}]^{3+}$ 2nd hydration sphere than to the central An^{III} subsystem. Gas phase binding energies for the h^{th} OH_2 ligand to the $[\text{An}^{\text{III}}(\text{OH}_2)_{h-1}]^{3+}$ fragment increase for $h = 8$ and 9 from 1.27 to 1.38 eV and from 1.15 to 1.23 eV, respectively. For the OH_2 dimer O_2H_4 , D_0 is found to be 0.10 eV at the BP86-DFT level of theory, using cc-pVQZ basis sets for O and H at fixed molecular structures optimized with aug-cc-pVDZ basis sets for O and H. Although experimental estimate [45] and CCSD(T) basis set limit values [46] are reported to be 0.23 and 0.22 eV, respectively, we assume that at the BP86-DFT level the $[\text{An}^{\text{III}}(\text{OH}_2)_{h-1}]^{3+}-\text{OH}_2$ interaction might be overestimated to some extent. At the MP2 level of theory, within the (7s6p5d2f)/[6s5p4d2f] An^{III} and O and H aug-cc-pVDZ basis sets, the h^{th} OH_2 ligand gas phase binding energies to the $[\text{An}^{\text{III}}(\text{OH}_2)_{h-1}]^{3+}$ fragment are found to increase for $h = 8$ from 1.25 to 1.36 eV, but are found to decrease for $h = 9$ from 1.09 to 0.91 eV for fixed BP86-DFT molecular structures, respectively; the corresponding O_2H_4 D_0 is 0.11 eV. Whereas the differences of BP86-DFT and MP2 gas phase binding energies for the h^{th} OH_2 ligand to the $[\text{An}^{\text{III}}(\text{OH}_2)_{h-1}]^{3+}$ fragment are generally small for $h = 8$, for $h = 9$, with increasing Z , the BP86-DFT binding energies are larger than MP2 binding energies by 0.06 to 0.32 eV. Therefore, and because of the similar O_2H_4 D_0 values at the BP86-DFT and MP2 level we assume the $[\text{An}^{\text{III}}(\text{OH}_2)_{h-1}]^{3+}-\text{OH}_2$ interaction to be somewhat overestimated by BP86-DFT, and, moreover, the extent of overestimation to increase with both h and Z .

The $[\text{An}^{\text{III}}(\text{OH}_2)_{h-1} \cdot \text{OH}_2]^{3+}$ hydration energies ΔE_{H} follow the same general trend as discussed for the $[\text{An}^{\text{III}}(\text{OH}_2)_h]^{3+}$ systems (cf. tab. III). Again, ΔE_{H} are similar for $h = 8$ and 9 . However, it is found that $[\text{An}^{\text{III}}(\text{OH}_2)_{h-1} \cdot \text{OH}_2]^{3+}$ SCRF energies are more positive

than the corresponding $[\text{An}^{\text{III}}(\text{OH}_2)_h]^{3+}$ SCRF energies, *i.e.*, the $[\text{An}^{\text{III}}(\text{OH}_2)_{h-1} \cdot \text{OH}_2]^{3+}$ systems are less stabilized in the COSMO SCRF than the $[\text{An}^{\text{III}}(\text{OH}_2)_h]^{3+}$ systems are. Again, SCRF energies are found to become more positive with increasing h . It is because of this that ΔE_{H} are more negative for $[\text{An}^{\text{III}}(\text{OH}_2)_8]^{3+}$ than for $[\text{An}^{\text{III}}(\text{OH}_2)_7 \cdot \text{OH}_2]^{3+}$, but more positive for $[\text{An}^{\text{III}}(\text{OH}_2)_9]^{3+}$ than for $[\text{An}^{\text{III}}(\text{OH}_2)_8 \cdot \text{OH}_2]^{3+}$.

Finally, An^{III} standard Gibbs free energies $\Delta G_{\text{H}}^{\circ}$ have been approximated from the calculated gas phase molecular structures and $[\text{An}^{\text{III}}(\text{OH}_2)_h]^{3+}$ hydration energies ΔE_{H} as

$$\Delta G_{\text{H}}^{\circ} \approx \Delta E_{\text{H}}^{\circ} - T\Delta S_{\text{H}}^{\circ} \approx \Delta E_{\text{H}} - T\Delta S^{\circ} \quad (3.4)$$

(cf. tab. I). The entropy change ΔS° is associated with the formation $\text{An}^{3+}(\text{g}) + h\text{OH}_2(\text{g}) \rightarrow [\text{An}^{\text{III}}(\text{OH}_2)_h]^{3+}(\text{g})$. $\Delta H_{\text{H}}^{\circ}$ has been approximated by ΔE_{H} because $\text{An}^{3+}(\text{g})$ H° data is neither available nor accessible from quantum chemistry calculations. As only gas phase molecular structures, and, therefore, only gas phase frequencies and moments of inertia have been calculated, one has to approximate $\Delta S_{\text{H}}^{\circ} \approx \Delta S^{\circ}$. Calculated ΔS° are negative and decrease with increasing h , which is expected since OH_2 coordination by An^{III} is a structure-making process. Compared to ΔE_{H} , $T\Delta S^{\circ}$ are small, so $\Delta G_{\text{H}}^{\circ}$ are dominated by the large negative ΔE_{H} and are thus found to be negative for all h and Z . However, since ΔE_{H} are similar for different h , the $T\Delta S^{\circ}$ contribution causes a trend inversion with respect to h , *i.e.*, $\Delta G_{\text{H}}^{\circ}$ is most negative for $h = 7$ and increases with increasing h . Generally, $\Delta G_{\text{H}}^{\circ}$ do not agree very well with reference An^{III} Gibbs free energies of hydration [38] for neither h . Because of the limited amount of An^{III} thermodynamic data reported, the different calculation schemes and the approximations involved, comparison of the calculated An^{III} $\Delta G_{\text{H}}^{\circ}$ is difficult. As the $\Delta G_{\text{H}}^{\circ}$ values are dominated by ΔE_{H} we feel, however, that the smooth decrease in An^{III} $\Delta G_{\text{H}}^{\circ}$ calculated by us might be connected with the 5f-in-core pseudopotential adjustment and the underlying average over a multitude of electronic states [24], whereas a 5f-in-valence approach allowing to treat only the ground state of each case would cause a slightly less regular behavior.

C. An^{III} preferred primary hydration numbers.

Finally, the question of An^{III} preferred primary hydration numbers will be addressed. Consider



the reaction energy ΔE being the difference of $[\text{An}^{\text{III}}(\text{OH}_2)_{h-1} \cdot \text{OH}_2]^{3+}$ and $[\text{An}^{\text{III}}(\text{OH}_2)_h]^{3+}$ hydration energies ΔE_{H} . For given Z , the preferred primary hydration number h^* is defined as the largest h that still yields $\Delta E < 0$. Generally, calculated h^* are both reasonable and consistent over the complete An^{III} series. ΔE increase with increasing Z for $h = 8$ and 9 from *ca.* -0.18 to -0.11 eV and from $+0.14$ to $+0.36$ eV, respectively. Thus, at least at the BP86-DFT level, $h^* = 8$ is predicted for all Z . This is found to be caused exclusively by the SCRF contributions to ΔE , since, for the corresponding gas phase reaction $[\text{An}^{\text{III}}(\text{OH}_2)_{h-1} \cdot \text{OH}_2]^{3+} (\text{g}) \longrightarrow [\text{An}^{\text{III}}(\text{OH}_2)_h]^{3+} (\text{g})$, ΔE increases with increasing Z for $h = 8$ and 9 from $+0.08$ to $+0.24$ eV and from $+0.25$ to $+0.53$ eV, respectively. As already discussed, for given h , COSMO SCRF energies are more negative for $[\text{An}^{\text{III}}(\text{OH}_2)_h]^{3+}$ than for $[\text{An}^{\text{III}}(\text{OH}_2)_{h-1} \cdot \text{OH}_2]^{3+}$ systems. For $h = 8$, it is only the gain in SCRF energy of $[\text{An}^{\text{III}}(\text{OH}_2)_8]^{3+}$ with respect to $[\text{An}^{\text{III}}(\text{OH}_2)_7 \cdot \text{OH}_2]^{3+}$ that compensates for the difference in gas phase binding energies, thus leading to preferred $h = 8$ with respect to $h = 7$. As COSMO SCRF contributions generally decrease with increasing h , this is not true any more for $h = 9$, *i.e.*, the gain in SCRF energy of $[\text{An}^{\text{III}}(\text{OH}_2)_9]^{3+}$ with respect to $[\text{An}^{\text{III}}(\text{OH}_2)_8 \cdot \text{OH}_2]^{3+}$ cannot compensate for the difference in gas phase binding energies, thus leading to preferred $h = 8$ with respect to $h = 9$. However, from this data one cannot come to a definite assignment of h^* to An^{III} because ΔE is quite small with respect to the systematical error expected.

As at the BP86-DFT level the $[\text{An}^{\text{III}}(\text{OH}_2)_{h-1}]^{3+} - \text{OH}_2$ interaction is overestimated with respect at the MP2 level, it is clear that at the MP2 level of theory An^{III} preferred primary hydration numbers h^* will be predicted to be somewhat larger. At the MP2 level, ΔE increase with increasing Z for $h = 8$ and 9 from *ca.* -0.40 to -0.35 eV and from -0.18 to $+0.03$ eV, respectively. Thus, $h^* = 9$ is predicted for Ac^{III}–Md^{III}, and $h^* = 8$ for No^{III} and Lr^{III} by 0.01 and 0.03 eV, respectively. This is because at the MP2 level SCRF energies are more negative for $[\text{An}^{\text{III}}(\text{OH}_2)_8]^{3+}$ than for $[\text{An}^{\text{III}}(\text{OH}_2)_7 \cdot \text{OH}_2]^{3+}$, and almost identical for $[\text{An}^{\text{III}}(\text{OH}_2)_9]^{3+}$ and $[\text{An}^{\text{III}}(\text{OH}_2)_8 \cdot \text{OH}_2]^{3+}$, whereas the $[\text{An}^{\text{III}}(\text{OH}_2)_{h-1}]^{3+} - \text{OH}_2$ interaction

energy is generally calculated *ca.* 0.10 eV lower than at the BP86-DFT level of theory.

IV. CONCLUSION.

We calculated gas phase molecular structures, binding energies, and, within a first-order approximation, hydration energies and Gibbs free energies of hydration of $[\text{An}^{\text{III}}(\text{OH}_2)_h]^{3+}$ for $h = 7, 8,$ and $9,$ using quasi-relativistic An^{III} 5f-in-core pseudopotentials at a DFT level of theory. Qualitatively, our calculations compare well with the general trends for the An^{III} series established from experimental [9–17] and computational studies [10, 19–21]. Serving as local models of bulk solvation effects, $[\text{An}^{\text{III}}(\text{OH}_2)_{h-1} \cdot \text{OH}_2]^{3+}$ gas phase $\text{An}^{\text{III}}-\text{O}$ distances of 1st sphere OH_2 ligands that coordinate a single 2nd shell OH_2 ligand come close to experimental data. The 5f-in-core approximation [24] appears to be applicable to $[\text{An}^{\text{III}}(\text{OH}_2)_h]^{3+}$ systems and, more general, has been demonstrated to be a powerful computational technique performing well with otherwise routine quantum chemistry density-functional theory methods.

Our calculations indicate that in the hydrated An^{III} species not less than 8 OH_2 ligands are directly coordinated to the An^{III} ion. A definite assignment of preferred primary hydration numbers h^* to An^{III} is difficult because of the very small energy differences ruling out one of the coordination isomers $[\text{An}^{\text{III}}(\text{OH}_2)_{h-1} \cdot \text{OH}_2]^{3+}$ and $[\text{An}^{\text{III}}(\text{OH}_2)_h]^{3+}$. There is evidence that at the BP86-DFT level $\text{An}^{\text{III}}-\text{OH}_2$ and $[\text{An}^{\text{III}}(\text{OH}_2)_{h-1}]^{3+}-\text{OH}_2$ interactions are somewhat ill-balanced, overestimating the interaction of 1st and 2nd hydration sphere OH_2 ligands. Moreover, h^* depends critically on the interplay between free OH_2 ligand, $[\text{An}^{\text{III}}(\text{OH}_2)_h]^{3+}$, and $[\text{An}^{\text{III}}(\text{OH}_2)_{h-1} \cdot \text{OH}_2]^{3+}$ SCRF energies. Therefore, we come to the conclusion that, for a more quantitative study of An^{III} hydration, one would have to carefully choose and apply a level of theory that better balances $\text{An}^{\text{III}}-\text{OH}_2$ interaction and the interaction of 1st and 2nd hydration sphere OH_2 ligands, and to carry out energy calculations within a most likely non-default, carefully parameterized PCM SCRF. Beside such technical aspects, our computational strategy to approach An^{III} can be systematically improved by considering molecular structure relaxation within the COSMO SCRF. $[\text{An}^{\text{III}}(\text{OH}_2)_h]^{3+}$ and $[\text{An}^{\text{III}}(\text{OH}_2)_{h-1} \cdot \text{OH}_2]^{3+}$ molecular structure optimization within the COSMO SCRF is in progress, but extremely difficult due to large numbers of high-order saddle-points near to the PES minima. In this context we wish to emphasize that it is absolutely necessary to confirm

the PES minimum nature of $[\text{An}^{\text{III}}(\text{OH}_2)_h]^{3+}$ molecular structures calculated. We believe that from $[\text{An}^{\text{III}}(\text{OH}_2)_h]^{3+}$ molecular structure optimizations within the COSMO SCRf one will come to a much more refined picture of An^{III} hydration. Computational studies of An^{III} aqueous chemistry, however, will remain a challenging subject.

V. ACKNOWLEDGMENTS.

We thank J. Held and the Regionales Rechenzentrum Köln (RRZK) for granting access to the RRZKs TURBOMOLE v. 5.7 program package.

VI. ELECTRONIC SUPPLEMENTARY MATERIAL

$[\text{An}^{\text{III}}(\text{OH}_2)_h]^{3+}$ ($h = 7, 8, 9$) and $[\text{An}^{\text{III}}(\text{OH}_2)_{h-1} \cdot \text{OH}_2]^{3+}$ ($h = 8, 9$) molecular structures, gas phase and COSMO SCRf total energies at BP86-DFT, MP2, and HF levels of theory, ZPEs, entropies, and An^{III} , O, and H Mulliken net charges.

-
- [1] W. F. Miller, *J. Chem. Edu.*, 1993, **70**(2), 109–114.
- [2] Energy, electricity and atomic power estimates for the period up to 2030 Technical Report IAEA-RDS-1/25, International Atomic Energy Agency, Wien, 2005.
- [3] G. R. Choppin, J. Liljenzin, and J. Rydberg, *Radiochemistry And Nuclear Chemistry*, Butterworth–Heinemann, Woburn, 3rd ed., 2002.
- [4] D. C. Hoffman and G. R. Choppin, *J. Chem. Edu.*, 1986, **63**(12), 1059–1064.
- [5] G. R. Choppin and K. L. Nash, *Radiochim. Acta*, 1995, **70–71**, 225–236.
- [6] Actinide separation chemistry in nuclear waste streams and materials Technical Report NEA/NSC/DOC(97)19, NEA/OECD, 1997.
- [7] R. J. Silva and H. Nitsche, *Radiochim. Acta*, 1995, **70–71**, 377–396.
- [8] J. J. Katz, G. T. Seaborg, and L. R. Morss, *The Chemistry Of The Actinide Elements*, Chapman and Hall Ltd., New York, 2nd ed., 1986.
- [9] F. David, B. Fourest, S. Hubert, J. F. Le Du, R. Revel, C. Den Auwer, C. Madic, L. R. Morss, G. Ionova, V. Mikhalko, V. Vokhmin, M. Nikonov, J. C. Berthet, and M. Ephritikhine In *Speciation, Techniques and Facilities for Radioactive Materials at Synchrotron Light Sources*, pp. 95–100, Grenoble, 4.–6. Oktober 1998, 1999. OECD/NEA.
- [10] M. R. Antonio, L. Soderholm, C. W. Williams, J.-P. Blaudeau, and B. E. Bursten, *Radiochim. Acta*, 2001, **89**, 17–25.
- [11] P. G. Allen, J. J. Bucher, D. K. Shuh, N. M. Edelstein, and T. Reich, *Inorg. Chem.*, 1997, **36**, 4676–4683.
- [12] P. G. Allen, J. J. Bucher, D. K. Shuh, N. M. Edelstein, and I. Craig, *Inorg. Chem.*, 2000, **39**, 595–601.
- [13] T. Stumpf, C. Hennig, A. Bauer, M. A. Denecke, and T. Fanghänel, *Radiochim. Acta*, 2004, **92**, 133–138.
- [14] M. R. Antonio, C. W. Williams, and L. Soderholm, *Radiochim. Acta*, 2002, **90**, 851–856.
- [15] R. Revel, C. Den Auwer, C. Madic, F. David, B. Fourest, S. Hubert, J.-F. Le Du, and L. R. Morss, *Inorg. Chem.*, 1999, **38**, 4139–4141.
- [16] T. Kimura, G. R. Choppin, Y. Kato, and Z. Yoshida, *Radiochim. Acta*, 1996, **72**, 61–64.
- [17] P. Lindqvist-Reis, R. Klenze, G. Schubert, and T. Fanghänel, *J. Phys. Chem. B*, 2005, **109**,

3077–3083.

- [18] H. Bertagnolli and T. S. Ertel, *Angew. Chem.*, 1994, **106**, 15–37.
- [19] Y. Mochizuki and S. Tsushima, *Chem. Phys. Lett.*, 2003, **372**, 114–102.
- [20] J.-P. Blaudeau, S. A. Zygmunt, L. A. Curtiss, D. T. Reed, and B. E. Bursten, *Chem. Phys. Lett.*, 1999, **310**, 347–354.
- [21] T. Yang and B. E. Bursten, *Inorg. Chem.*, 2006, **45**, 5291–5301.
- [22] Y. Mochizuki and H. Tatewaki, *Chem. Phys.*, 2001, **273**, 135–148.
- [23] Y. Mochizuki and H. Tatewaki, *J. Chem. Phys.*, 2002, **116**(20), 8838–8842.
- [24] A. Moritz, X. Cao, and M. Dolg, *Theor. Chem. Acc.*
- [25] A. Klamt, V. Jonas, T. Bürger, and J. C. W. Lohrenz, *J. Phys. Chem. A*, 1998, **102**, 5074–5085.
- [26] A. Klamt and G. Schüürmann, *J. Chem. Soc. Perkin Trans.*, 1993, **2**, 799–805.
- [27] C. Clavaguéra-Sarrio, V. Vallet, D. Maynau, and C. J. Marsden, *J. Chem. Phys.*, 2004, **121**(11), 5312–5321.
- [28] R. Ahlrichs, M. Bär, M. Häser, H. Horn, and C. Kölmel, *Chem. Phys. Lett.*, 1989, **162**, 165–169.
- [29] T. H. Dunning Jr., *J. Chem. Phys.*, 1988, **90**(2), 1007–1023.
- [30] J. Wiebke, Hydratation der dreiwertigen Ionen der Actinoide Master’s thesis, 2006.
- [31] P. A. M. Dirac, *Proc. Camb. Phil. Soc.*, 1930, **26**, 376–385.
- [32] A. Becke, *Phys. Rev. A*, 1988, **38**(6), 3098–3100.
- [33] J. P. Perdew, *Phys. Rev. B*, 1986, **33**(12), 8822–8824.
- [34] J. C. Slater, *Phys. Rev.*, 1951, **81**, 385–390.
- [35] S. H. Vosko, L. Wilk, and M. Nusair, *Can. J. Phys.*, 1980, **58**, 1200–1211.
- [36] J. Neugebauer and B. A. Hess, *J. Chem. Phys.*, 2003, **118**(16), 7215–7225.
- [37] R. D. Loss, *Pure Appl. Chem.*, 2003, **75**(8), 1107–1122.
- [38] H. F. David and V. Vokhmin, *New J. Chem.*, 2003, **27**, 1627–1632.
- [39] C. Cossy, L. Helm, D. H. Powell, and A. E. Merbach, *New J. Chem.*, 1995, **19**, 27–35.
- [40] T. Kowall, F. Foglia, L. Helm, and A. E. Merbach, *J. Phys. Chem.*, 1995, **99**, 13078–13087.
- [41] U. Cosentino, G. Moro, D. Pitea, L. Calabi, and A. Maiocchi, *J. Mol. Struct. THEOCHEM*, 1997, **392**, 75–85.
- [42] U. Cosentino, A. V. an D. Pitea, G. Moro, and V. Barone, *J. Phys. Chem. B*, 2000, **104**,

8001–8007.

- [43] J. K. Laerdahl, K. Faegri Jr., L. Visscher, and T. Saue, *J. Chem. Phys.*, 1998, **109**(24), 10806–10817.
- [44] G. A. Krestov, *Thermodynamics Of Solvation*, Ellis Horwood Ltd., Chichester, 1991.
- [45] L. A. Curtiss, D. J. Frurip, and M. Blander, *J. Chem. Phys.*, 1979, **71**(1), 2703–2711.
- [46] A. Halkier, H. Koch, P. Jørgensen, O. Christansen, I. M. Beck Nielsen, and T. Helgaker, *Theor. Chim. Acc.*, 1997, **97**, 150–157.

TABLE I: An^{III} PCM cavity radii r (in pm), Gibbs free energies of hydration $\Delta G_{\text{H}}^{\circ}$ (in kJ mol⁻¹) for different h , and reference An^{III} Gibbs free energies of hydration (in kJ mol⁻¹).

	r	$\Delta G_{\text{H}}^{\circ}$			$\Delta G_{\text{H}}^{\circ}$ [38]
		$h = 7$	$h = 8$	$h = 9$	
Ac	224	-2831	-2810	-2791	-2806
Th	217	-2871	-2858	-2832	-2885
Pa	215	-2908	-2894	-2865	-2921
U	206	-2925	-2931	-2902	-3045
Np	204	-2980	-2965	-2937	-3073
Pu	200	-3011	-2998	-2966	-3134
Am	199	-3042	-3029	-2994	-3159
Cm	195	-3073	-3061	-3027	-3225
Bk	188	-3100	-3088	-3053	-3340
Cf	182	-3130	-3119	-3081	-3444
Es	179	-3155	-3144	-3106	-3498
Fm	177	-3180	-3168	-3128	-3546
Md	175	-3207	-3195	-3150	-3585
No	173	-3232	-3219	-3173	-3623
Lr	172	-3257	-3244	-3200	-3644

TABLE II: Mean An^{III}-O distances d_{AnO} for $[\text{An}^{\text{III}}(\text{OH}_2)_h]^{3+}$, and mean An^{III}-O distances d_{AnO} for $[\text{An}^{\text{III}}(\text{OH}_2)_{h-1} \cdot \text{OH}_2]^{3+}$ 1st hydration sphere OH₂ ligands that coordinate the 2nd hydration sphere OH₂ ligand (in pm).

	$[\text{An}^{\text{III}}(\text{OH}_2)_h]^{3+}$			$[\text{An}^{\text{III}}(\text{OH}_2)_{h-1} \cdot \text{OH}_2]^{3+}$	
	$h = 7$	$h = 8$	$h = 9$	$h = 8$	$h = 9$
Ac	263.4	266.5	269.9	257.6	258.9
Th	261.3	264.3	268.2	255.6	258.7
Pa	259.1	262.2	265.6	253.5	250.8
U	256.9	260.1	263.6	251.4	254.6
Np	254.8	258.0	261.7	249.4	252.6
Pu	252.9	256.1	259.9	247.6	250.8
Am	251.1	254.4	258.2	245.7	249.1
Cm	249.3	252.6	256.6	244.0	247.3
Bk	247.7	251.1	255.1	242.6	245.8
Cf	246.0	249.5	253.7	241.0	244.2
Es	244.7	248.2	252.4	239.6	242.9
Fm	243.3	246.9	251.3	238.3	241.6
Md	241.9	245.5	250.2	236.9	240.3
No	240.6	244.3	249.0	235.7	239.0
Lr	239.3	243.1	247.8	234.5	237.9

TABLE III: Negative gas phase binding energies $-D_0$ (first value) and differences in SCRF stabilization energies $\Delta E^{\text{SCRF}} < 0$ (second value) for $[\text{An}^{\text{III}}(\text{OH}_2)_h]^{3+}$ and $[\text{An}^{\text{III}}(\text{OH}_2)_{h-1} \cdot \text{OH}_2]^{3+}$ (in eV). Both values sum up to the hydration energies $\Delta E_{\text{H}} \approx -D_0 + \Delta E^{\text{SCRF}}$ as defined in eq. 3.3 and plotted in fig. 5. For the free OH_2 system the SCRF stabilization energy is $E_{\text{OH}_2}^{\text{SCRF}} = -0.30$ eV,

	$[\text{An}^{\text{III}}(\text{OH}_2)_h]^{3+}$			$[\text{An}^{\text{III}}(\text{OH}_2)_{h-1} \cdot \text{OH}_2]^{3+}$	
	$h = 7$	$h = 8$	$h = 9$	$h = 8$	$h = 9$
Ac	-16.66 - 16.96	-17.85 - 16.26	-18.74 - 15.91	-17.93 - 16.11	-18.99 - 15.80
Th	-17.01 - 17.00	-18.20 - 16.42	-19.09 - 15.96	-18.29 - 16.15	-19.35 - 15.84
Pa	-17.35 - 17.04	-18.55 - 16.46	-19.43 - 16.02	-18.64 - 16.19	-19.71 - 15.92
U	-17.69 - 16.90	-18.89 - 16.51	-19.77 - 16.07	-18.99 - 16.22	-20.06 - 16.02
Np	-18.02 - 17.15	-19.21 - 16.56	-20.08 - 16.12	-19.33 - 16.29	-20.39 - 16.02
Pu	-18.32 - 17.18	-19.52 - 16.61	-20.37 - 16.17	-19.65 - 16.33	-20.70 - 16.07
Am	-18.63 - 17.21	-19.81 - 16.66	-20.64 - 16.22	-19.96 - 16.36	-21.00 - 15.96
Cm	-18.93 - 17.24	-20.12 - 16.69	-20.93 - 16.25	-20.26 - 16.40	-21.31 - 16.00
Bk	-19.19 - 17.26	-20.37 - 16.73	-21.17 - 16.29	-20.53 - 16.43	-21.58 - 16.16
Cf	-19.47 - 17.30	-20.66 - 16.76	-21.43 - 16.33	-20.82 - 16.44	-21.86 - 16.19
Es	-19.72 - 17.32	-20.89 - 16.80	-21.66 - 16.37	-21.07 - 16.48	-22.10 - 16.22
Fm	-19.95 - 17.36	-21.12 - 16.83	-21.87 - 16.40	-21.31 - 16.51	-22.33 - 16.25
Md	-20.21 - 17.39	-21.37 - 16.88	-22.10 - 16.43	-21.58 - 16.54	-22.59 - 16.17
No	-20.45 - 17.41	-21.60 - 16.90	-22.31 - 16.47	-21.82 - 16.57	-22.82 - 16.20
Lr	-20.68 - 17.44	-21.83 - 16.93	-22.53 - 16.51	-22.07 - 16.59	-23.06 - 16.34

- Fig. 1** Schematical representation of the computational strategy to approach An^{III} hydration.
- Fig. 2** $[\text{An}^{\text{III}}(\text{OH}_2)_h]^{3+}$ and $[\text{An}^{\text{III}}(\text{OH}_2)_{h-1} \cdot \text{OH}_2]^{3+}$ gas phase molecular structures. **1**, **2**, and **3** have 7, 8, and 9 OH_2 ligands in the 1st, **4** and **5** have 7 and 8 OH_2 ligands in the 1st and one OH_2 ligand in the 2nd hydration shell, respectively.
- Fig. 3** Mean gas phase $\text{An}^{\text{III}}\text{-O}$ distances d_{AnO} for $[\text{An}^{\text{III}}(\text{OH}_2)_h]^{3+}$ systems; d_{AnO} rms given refer to deviations of non-symmetry equivalent $\text{An}^{\text{III}}\text{-O}$ distances from the total average. Experimental d_{AnO} and rms are from EXAFS [9–15] and TRLF spectroscopy [16, 17].
- Fig. 4** An^{III} Mulliken net charges in $[\text{An}^{\text{III}}(\text{OH}_2)_h]^{3+}$ for primary hydration numbers h of 7, 8, and 9. An^{III} 5f Mulliken populations decrease from 0.14 to 0.05 with increasing Z (cf. electronic supplementary information).
- Fig. 5** An^{III} hydration energies $\Delta E_{\text{H}} \approx -D_0 + \Delta E^{\text{SCRF}}$, calculated for $[\text{An}^{\text{III}}(\text{OH}_2)_h]^{3+}$ and primary hydration numbers h of 7, 8, and 9. Note that for Md^{III} , No^{III} , and Lr^{III} the calculated ΔE_{H} values are slightly more negative for $h = 8$ than for $h = 9$.

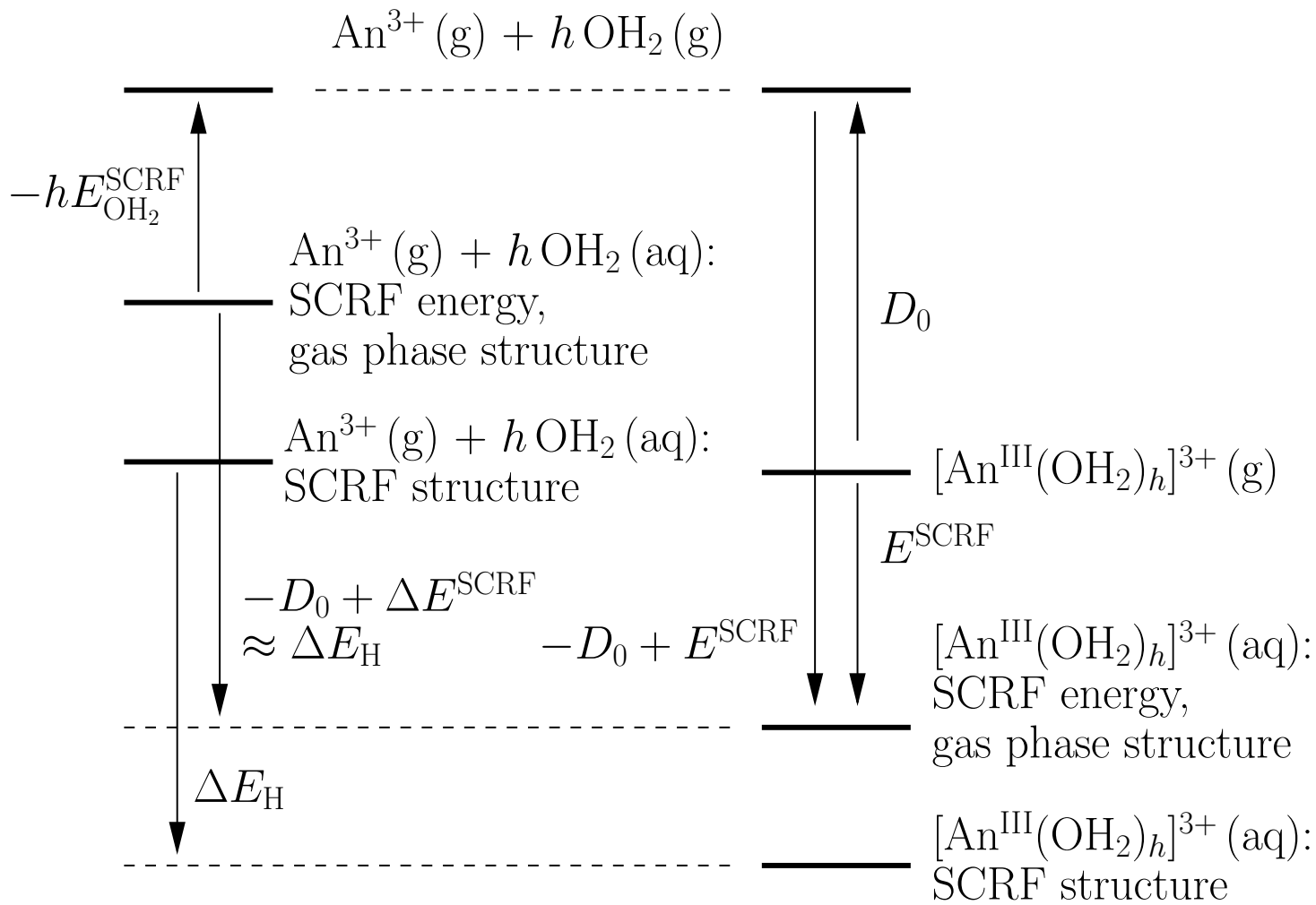


FIG. 1: Schematical representation of the computational strategy to approach An^{III} hydration.

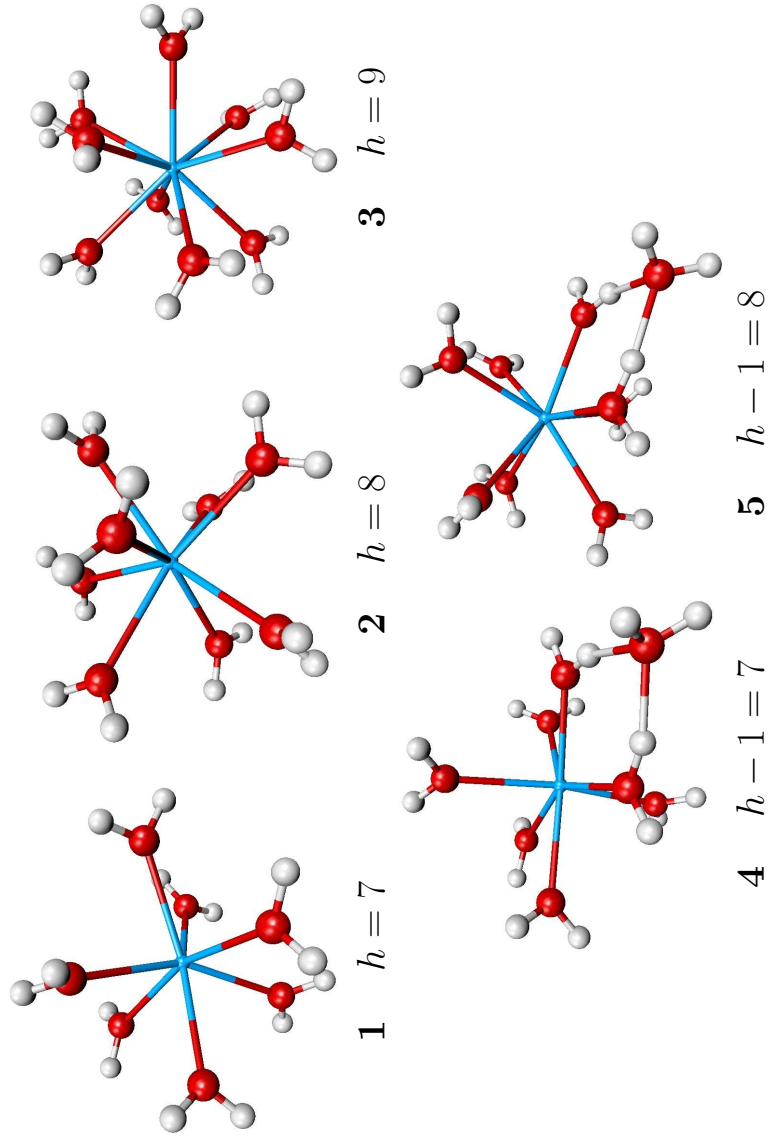


FIG. 2: $[\text{An}^{\text{III}}(\text{OH}_2)_h]^{3+}$ and $[\text{An}^{\text{III}}(\text{OH}_2)_{h-1} \cdot \text{OH}_2]^{3+}$ gas phase molecular structures. **1**, **2**, and **3** have 7, 8, and 9 OH_2 ligands in the 1st, **4** and **5** have 7 and 8 OH_2 ligands in the 1st and one OH_2 ligand in the 2nd hydration shell, respectively.

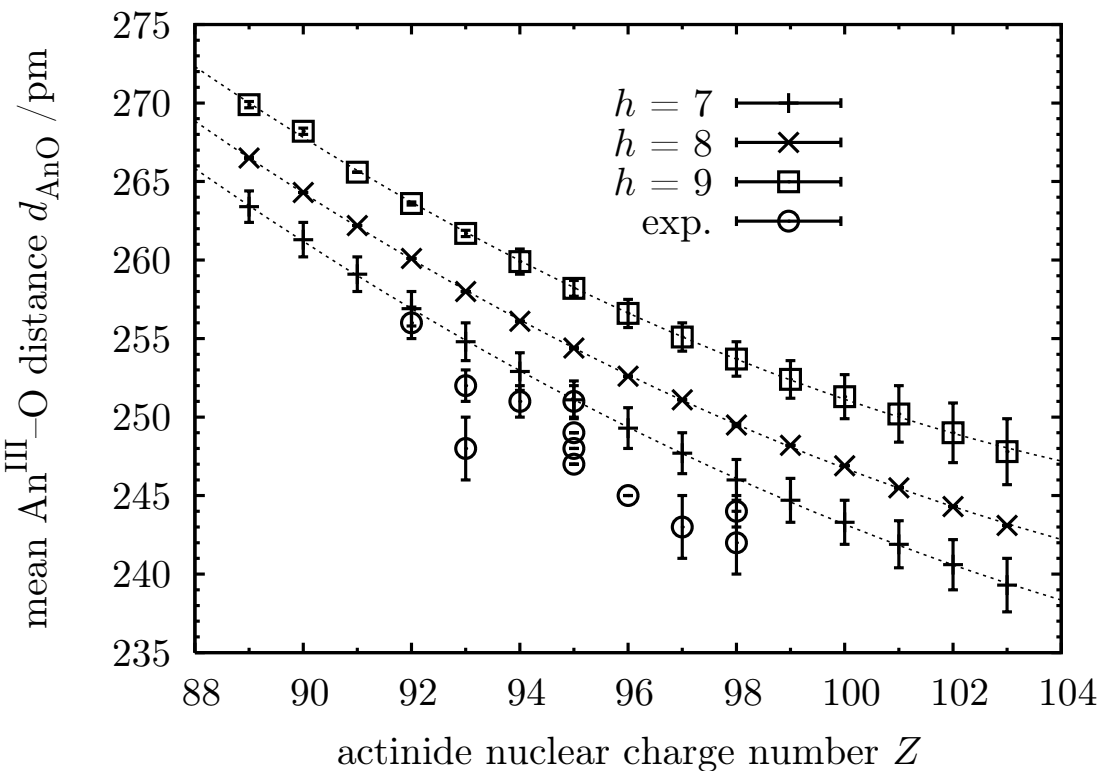


FIG. 3: Mean gas phase $\text{An}^{\text{III}}\text{O}$ distances d_{AnO} for $[\text{An}^{\text{III}}(\text{OH}_2)_h]^{3+}$ systems; d_{AnO} rms given refer to deviations of non-symmetry equivalent $\text{An}^{\text{III}}\text{O}$ distances from the total average. Experimental d_{AnO} and rms are from EXAFS [9–15] and TRLF spectroscopy [16, 17].

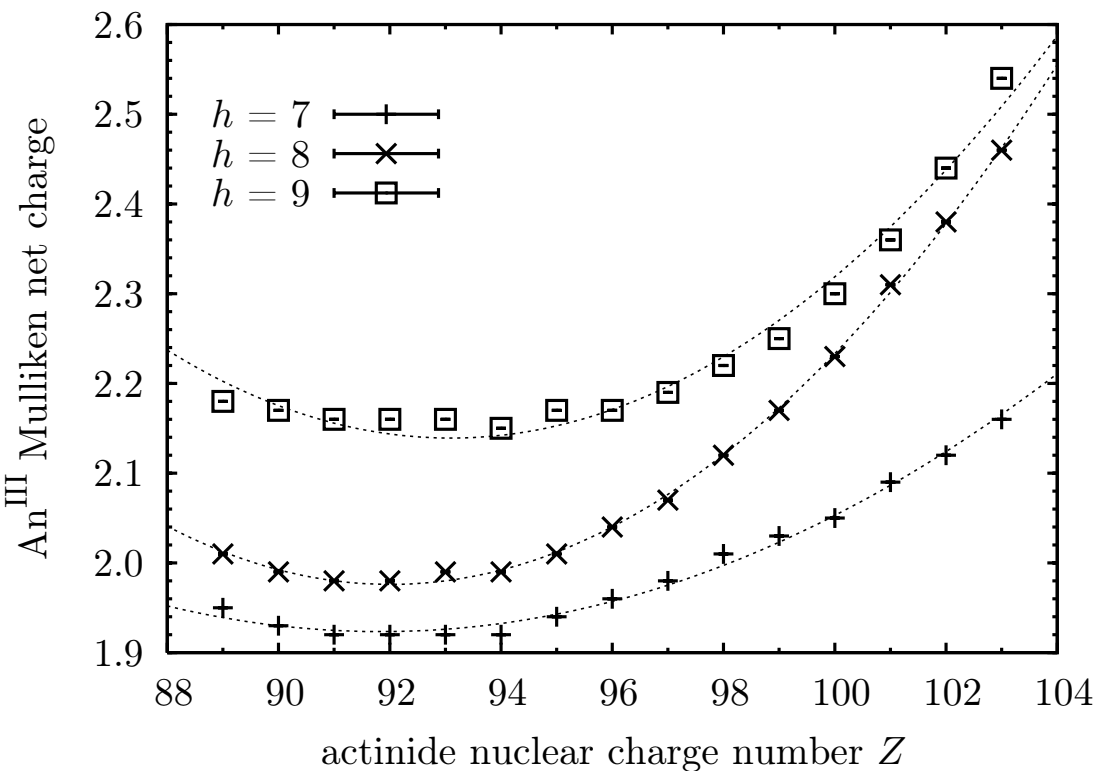


FIG. 4: An^{III} Mulliken net charges in [An^{III}(OH₂)_h]³⁺ for primary hydration numbers h of 7, 8, and 9. An^{III} 5f Mulliken populations decrease from 0.14 to 0.05 with increasing Z (cf. electronic supplementary information).

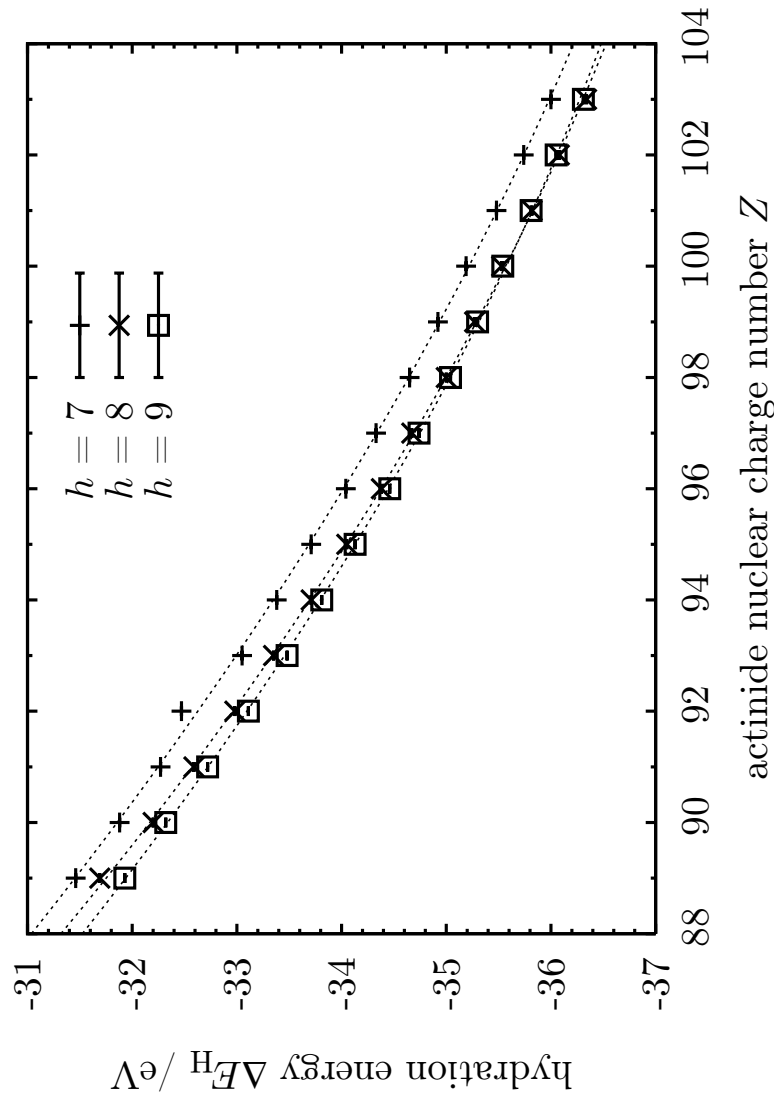


FIG. 5: An^{III} hydration energies $\Delta E_{\text{H}} \approx -D_0 + \Delta E^{\text{SCRFF}}$, calculated for $[\text{An}^{\text{III}}(\text{OH}_2)_h]^{3+}$ and primary hydration numbers h of 7, 8, and 9. Note that for Md^{III} , No^{III} , and Lr^{III} the calculated ΔE_{H} values are slightly more negative for $h = 8$ than for $h = 9$.